Supplemental Material

Concomitant SK Current Activation and Sodium Current Inhibition Cause J Wave Syndrome

M. Chen, D.Z. Xu, A.Z. Wu, S. Guo, J. Wan, D. Yin, S.F. Lin, Z. Chen, M. Rubart, T.H. Everett, Z. Qu, J.N. Weiss, P.S. Chen
Correspondence to: chenpp@iu.edu

Supplemental Figures and Tables

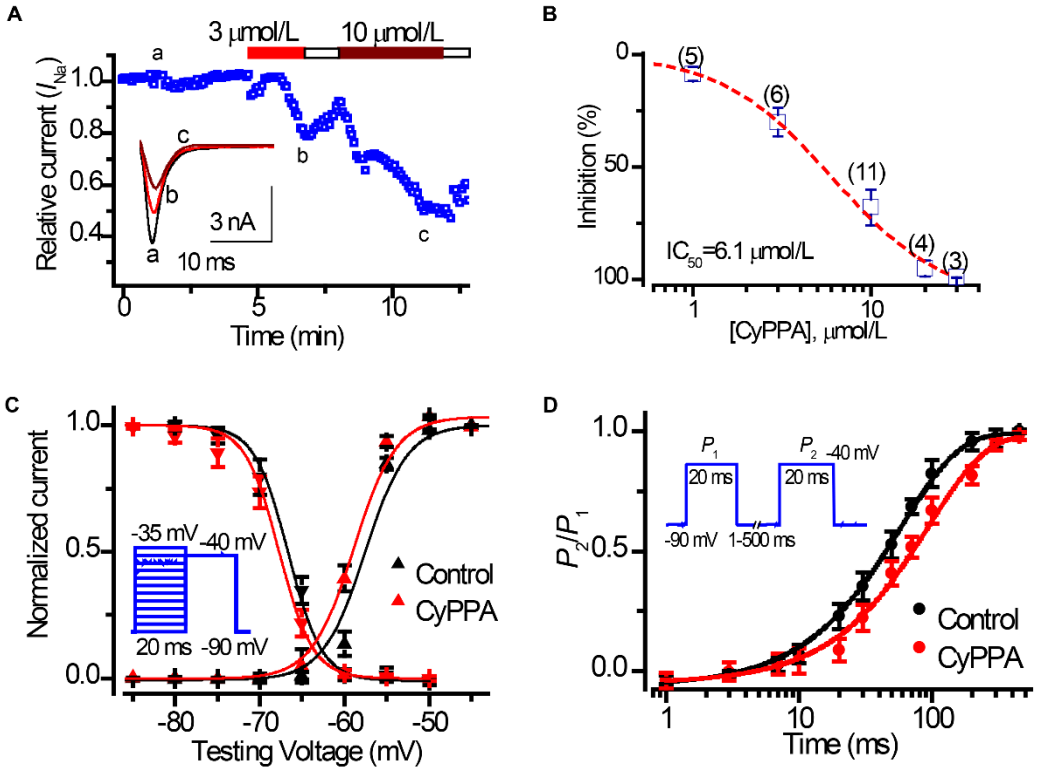

Supplemental Figure 1. Effects of CyPPA on sodium current (I_{Na}) properties. A. Time course of change in the normalized I_{Na} during the bath application of CyPPA (red bar) and washout (white bar). The current traces were recordings of (a) control, (b) 3 μmol/L and (c)10 μmol/L CyPPA (red traces) application, respectively. **B.** Relationship between the percentage inhibition of normalized I_{Na} and CyPPA concentration. The smooth line represents the best fit to a Hill function (n=3-11 in each point). The values for IC_{50}, maximally decreased percentage of I_{Na} and the Hill coefficient were 6.1 μmol/L, 100% and 1.0, respectively. **C.** Effects of CyPPA (10 μmol/L) on the activation and steady-state inactivation, as well as the recovery rate of I_{Na} from slow inactivation (**D,** each n=6). The paired-pulse protocols shown as insets in the relative graphs. Each point represents the mean ± SEM.

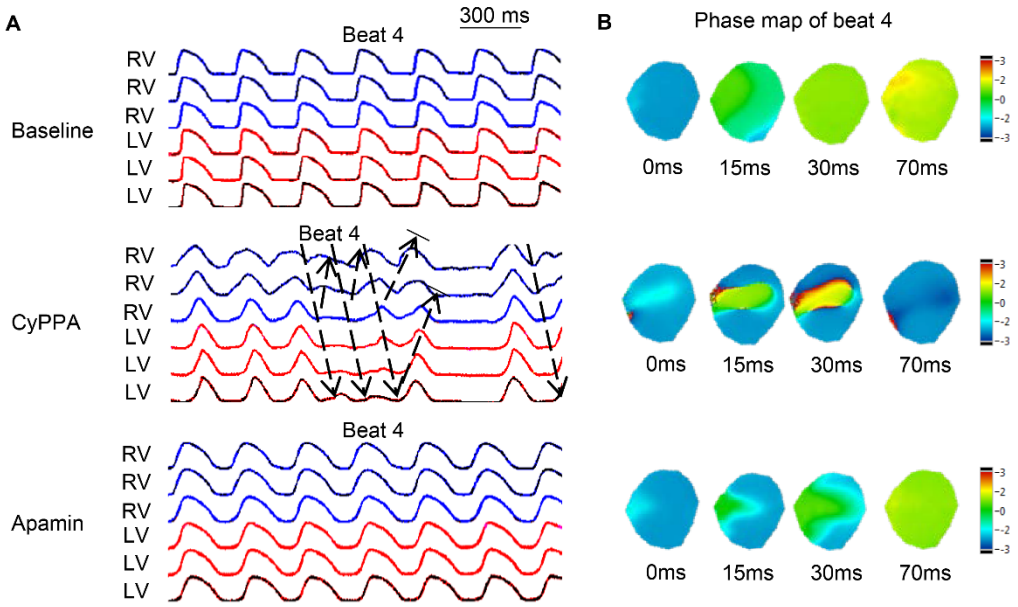

Supplemental Figure 2. Pacing-induced phase 2 reentry (P2R) after CyPPA. A. Representative V_m traces at pacing cycle length 300 ms (Protocol I). Pacing 1:1 captured the ventricles at baseline. CyPPA triangulated action potential (AP) with slow depolarization and fast repolarization at early phases, and enlarged AP dispersions prior to the onset of pacing-induced arrhythmias. P2R (beat 4) was induced which originated from the right ventricle (RV) and propagated to the left ventricle (LV). Apamin prolonged action potential duration (APD), restored AP plateau and reduced APD heterogeneity. **B.** Phase maps of beat 4 display normal activation at baseline and after apamin. After CyPPA, wavebreaks occurred and quickly degenerated into reentry.

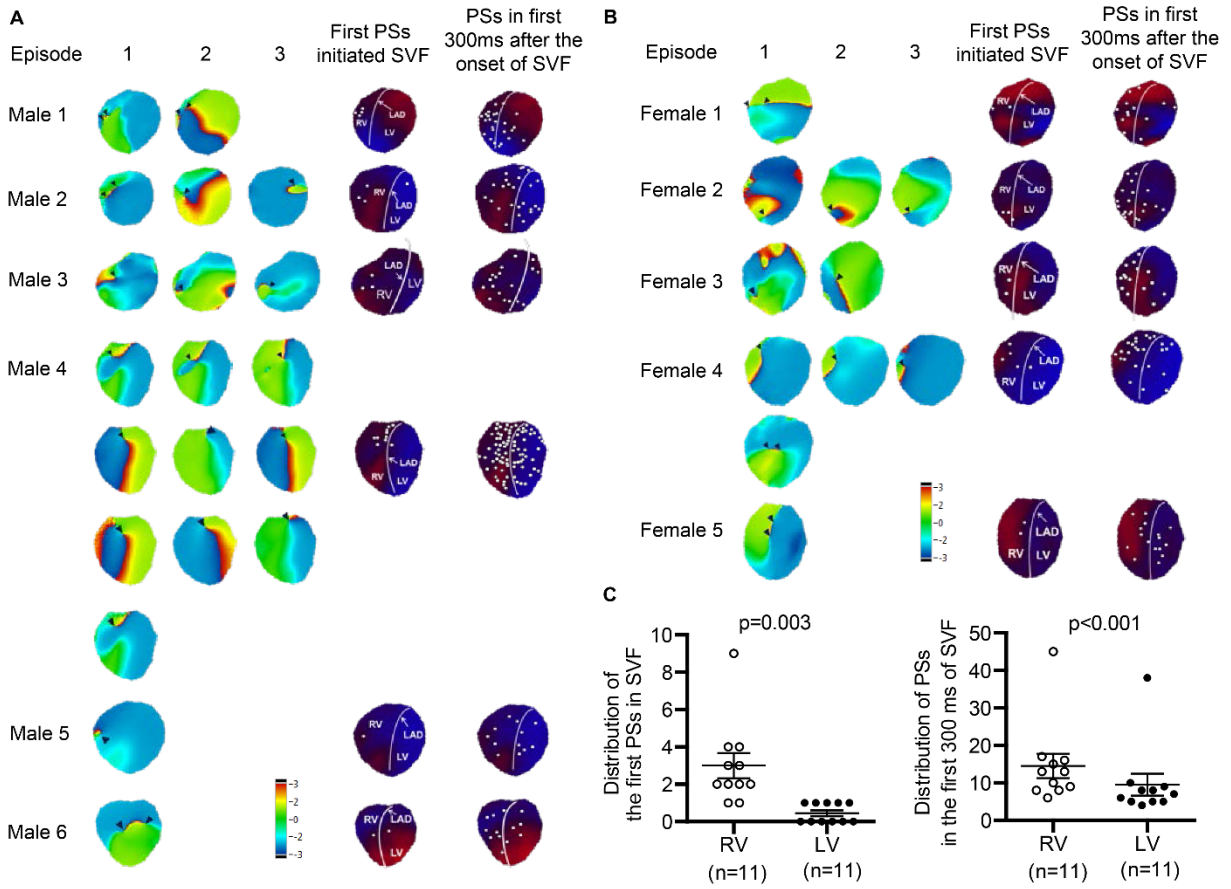

Supplemental Figure 3. Distributions of phase singularities (PSs) in CyPPA-induced spontaneous ventricular fibrillation (SVF). Phase maps show the PSs (arrowhead) which initiated each episode of SVF captured by optical mapping in **(A)** 6 males and **(B)** 5 females. First PSs at the initiation of SVF and PSs in the first 300ms after the onset of SVF were plotted on the right columns with white dots. Note that PSs were more frequently distributed in the right ventricles (RV) than in the left ventricles (LV). **C.** Significant differences existed in the PS distributions between the RV and the LV. Data represent mean ± SEM. Statistical significance was determined by paired t test.

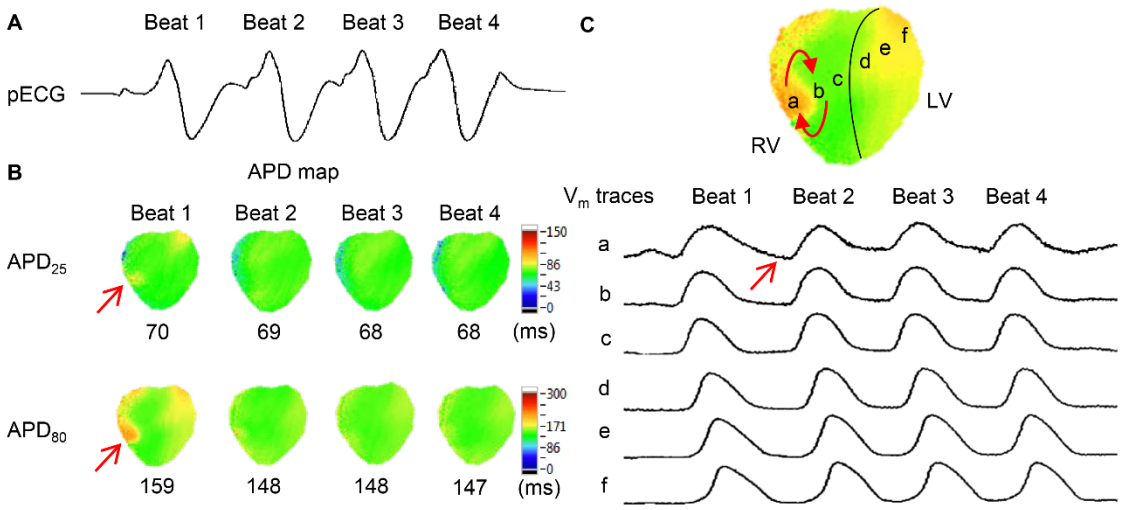

Supplemental Figure 4. Non-sustained ventricular tachycardia (NSVT) induced by CyPPA. **A.** Representative pECG trace of an episode of spontaneous NSVT after CyPPA. **B.** Action potential duration (APD_{25}) and APD_{80} maps. Large APD gradient in the right ventricle (RV) preceded the beat initiating NSVT (red arrows). **C.** V_m traces at different sites of the ventricles. Beat 1 exhibited large APD gradient between the adjacent sites (site **a** and site **b**, red arrow) in the RV, thus initiating the reentry.

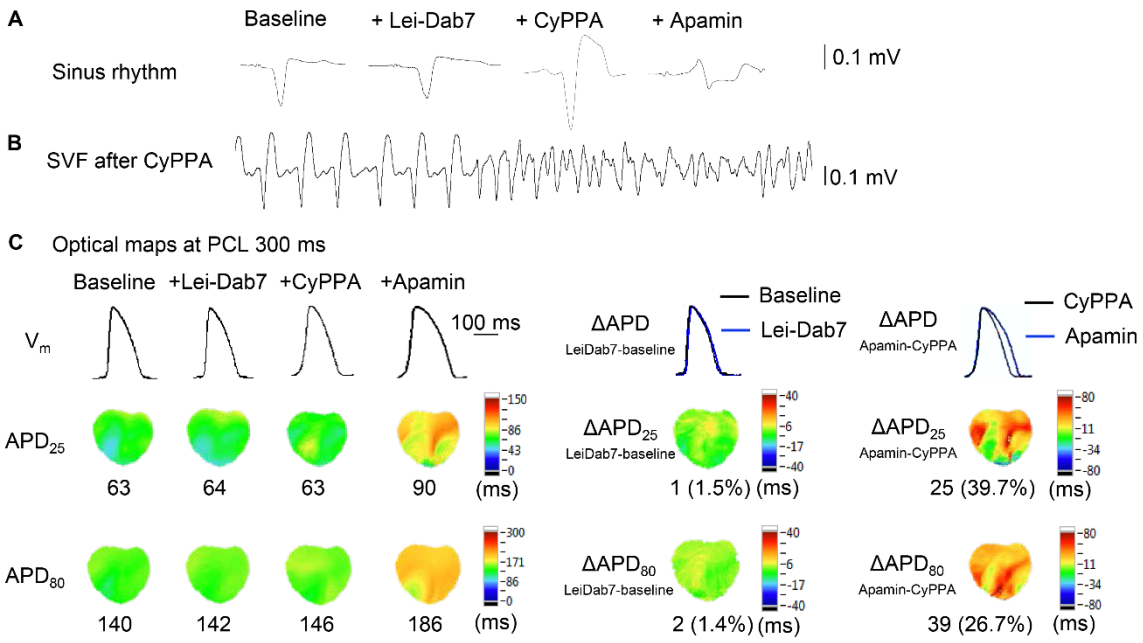

Supplemental Figure 5. Effects of CyPPA in the presence of SK2 blockade. Representative pECG and optical maps at baseline, after Lei-Dab7, after CyPPA and after apamin (Protocol IIa, n=3). **A.** pECG during sinus rhythm shows no prominent J wave at baseline and after Lei-Dab7. With SK2 blockade by Lei-Dab7 pretreatment, CyPPA still accentuated J wave. Subsequent SK3 blockade by apamin suppressed J wave. **B.** pECG exhibits an episode of spontaneous ventricular fibrillation (SVF) after CyPPA. No SVF was observed at baseline, after Lei-Dab7 and after apamin. **C.** Optical maps at pacing cycle length (PCL) 300ms. Compared with baseline, Lei-Dab7 did not prolonged action potential duration (APD, less than 5%). Compared with CyPPA, apamin prolonged both APD_{25} and APD_{80} and more prominently and heterogeneously at APD_{25}.

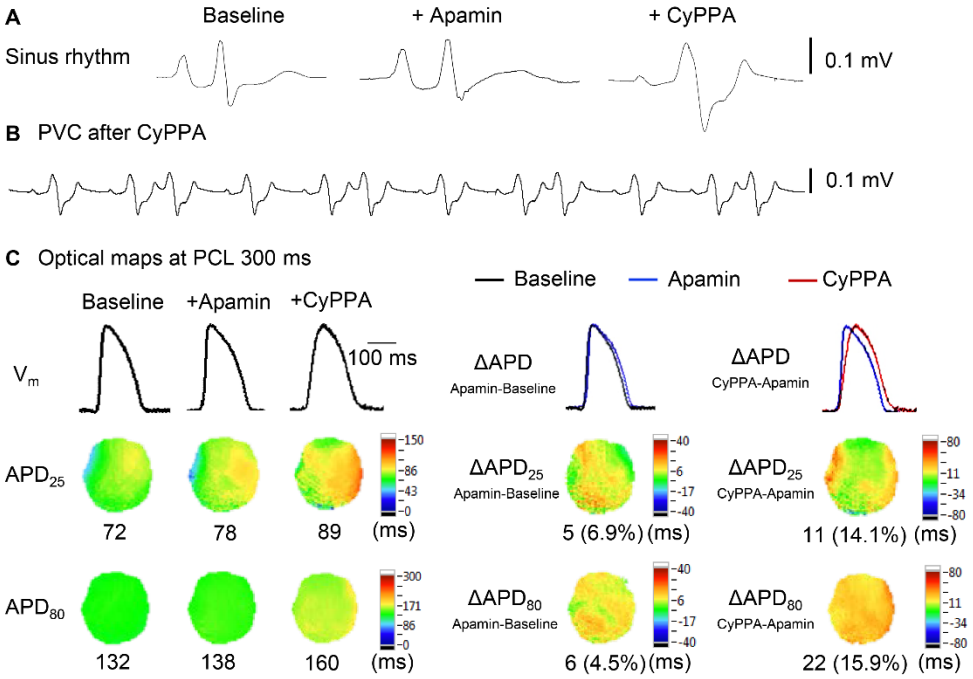

Supplemental Figure 6. Effects of CyPPA in the presence of both SK2 and SK3 blockade. Representative pECG and optical maps at baseline, after apamin and after CyPPA (Protocol IIb, n=3). **A.** pECG during sinus rhythm exhibits no prominent J wave at baseline, after apamin and after CyPPA. **B.** Spontaneous premature ventricular contractions (PVCs) were frequently observed after CyPPA, however, none of them degenerated into ventricular fibrillation. **C.** Optical maps at pacing cycle length (PCL) 300ms. Compared with baseline, apamin only slightly prolonged action potential duration (APD, about 5%). With apamin pretreatment, CyPPA decelerated action potential upstroke which prolonged APD.

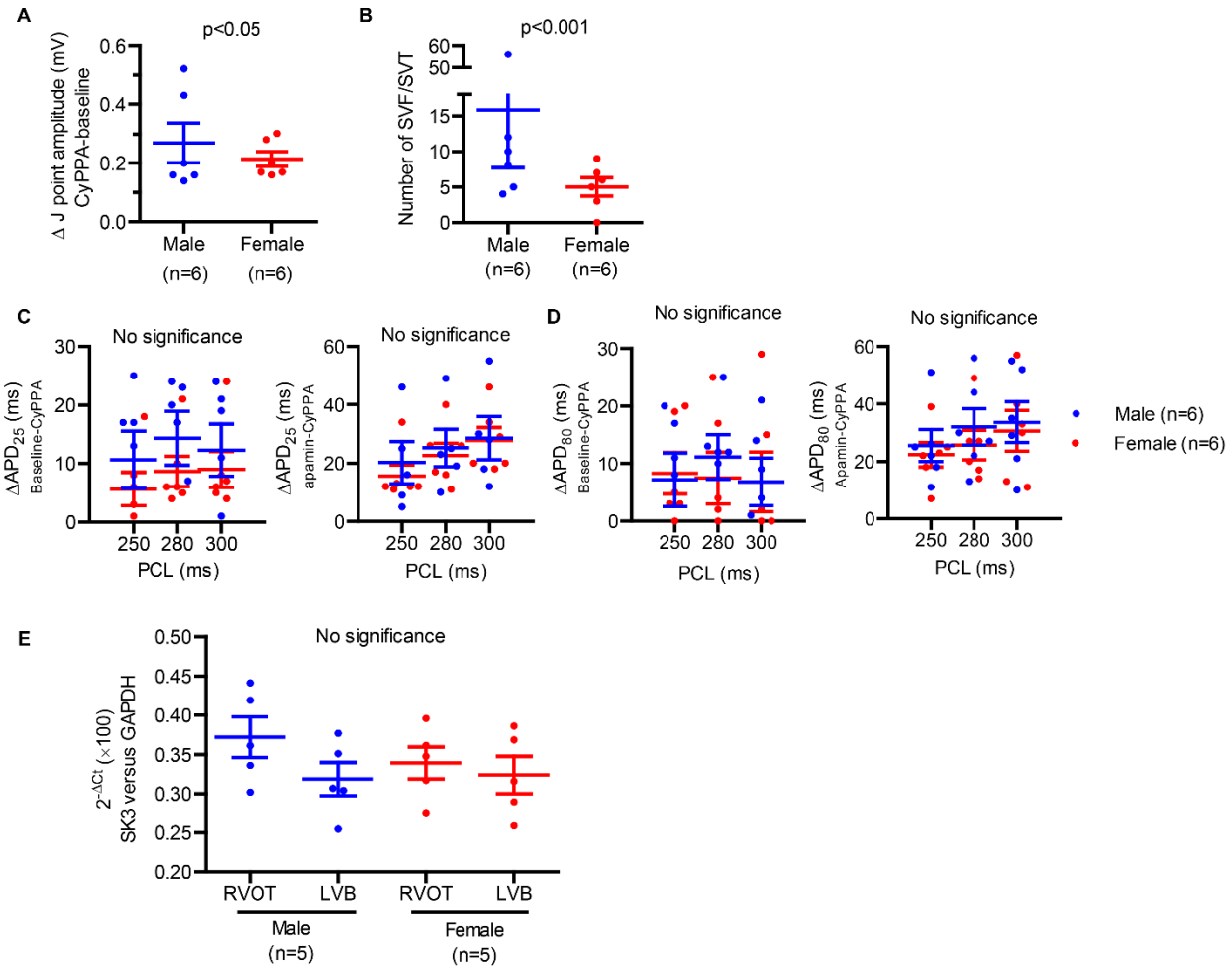

Supplemental Figure 7. Sex and regional differences. A. CyPPA-induced J point amplitude elevation (Δ J point amplitude) was significantly larger in males than in females. **B.** The frequency of spontaneous ventricular fibrillation (SVF) or spontaneous ventricular tachycardia (SVT) was significantly higher in males than in females. (For A and B: mean ± SEM, unpaired t-tests) **C.** The average values of action potential duration (APD_{25}) shortening after CyPPA and APD_{25} prolongation after apamin were larger in males than in females, but without statistical significance. **D.** APD_{80} shortening after CyPPA and APD_{80} prolongation after apamin were similar in males and females. (For C and D: mean ± SEM, two-way ANOVA with Bonferroni post-tests) **E.** qPCR measuring the RNA expression of SK3 (*Kcnn3*) in ventricular tissue preparations dissected from the right ventricular outflow tract (RVOT) and left ventricular base (LVB) of 5 males and 5 females. The results have been normalized to the expression of the housekeeper gene GAPDH in the same preparation pools. There was no significant difference among all comparisons (Mean ± SEM, one-way ANOVA with Tukey post-tests).

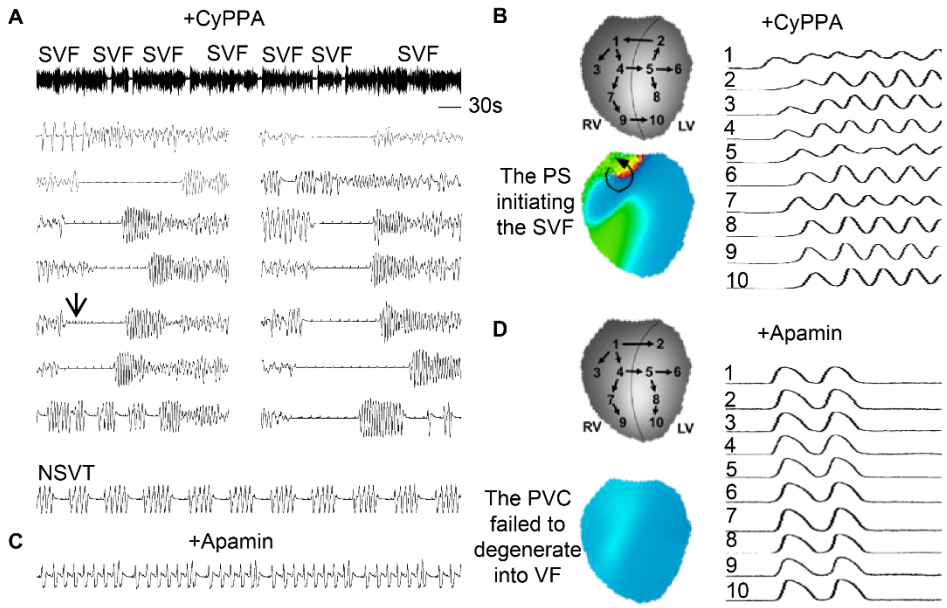

Supplemental Figure 8. I_{KAS} blockade is antiarrhythmic in CyPPA-induced J wave syndrome. A. CyPPA induced electrical storm (ES) in a male rabbit. Non-sustained ventricular tachycardia (NSVT), atrioventricular block and atrial tachycardia (arrow) were also observed after CyPPA. **B.** Representative V_m traces and phase map at the onset of spontaneous ventricular fibrillation (SVF) after CyPPA. SVF was initiated from the right ventricular outflow tract (RVOT, site 1). The activation sequence of reentry was 1-4-5-2-1. Other parts of the ventricles were activated passively. **C.** ES was terminated after apamin administration. Although spontaneous premature ventricular contractions (PVCs) were still frequently observed, none of them degenerated into SVF. **D.** Representative V_m traces and phase map of PVC after apamin. The PVC originated from the similar region of the RVOT (site 1) but failed to complete the reentry.

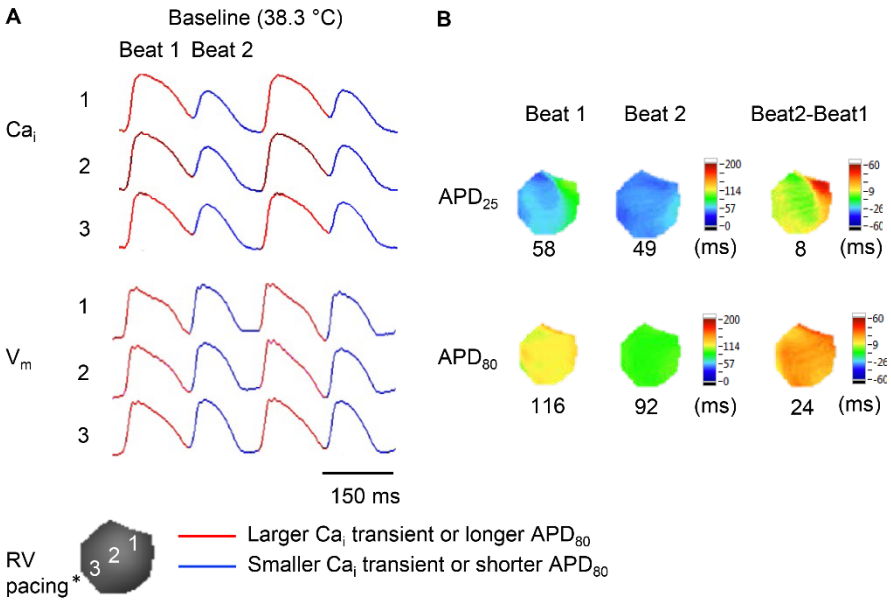

Supplemental Figure 9. Positive coupling and spatial concordance of Ca_i and V_m alternans during normothermia. A. At normal body temperature (38.3 °C), Ca_i and V_m alternans were induced by ventricular pacing at 150 ms. Ca_i and V_m were positively coupled at both proximal and distal sites, leading to spatially concordant alternans. **B.** APD maps show the differences between two consecutive beats (beat 2-beat 1) were smaller at APD_{25} than at APD_{80}.

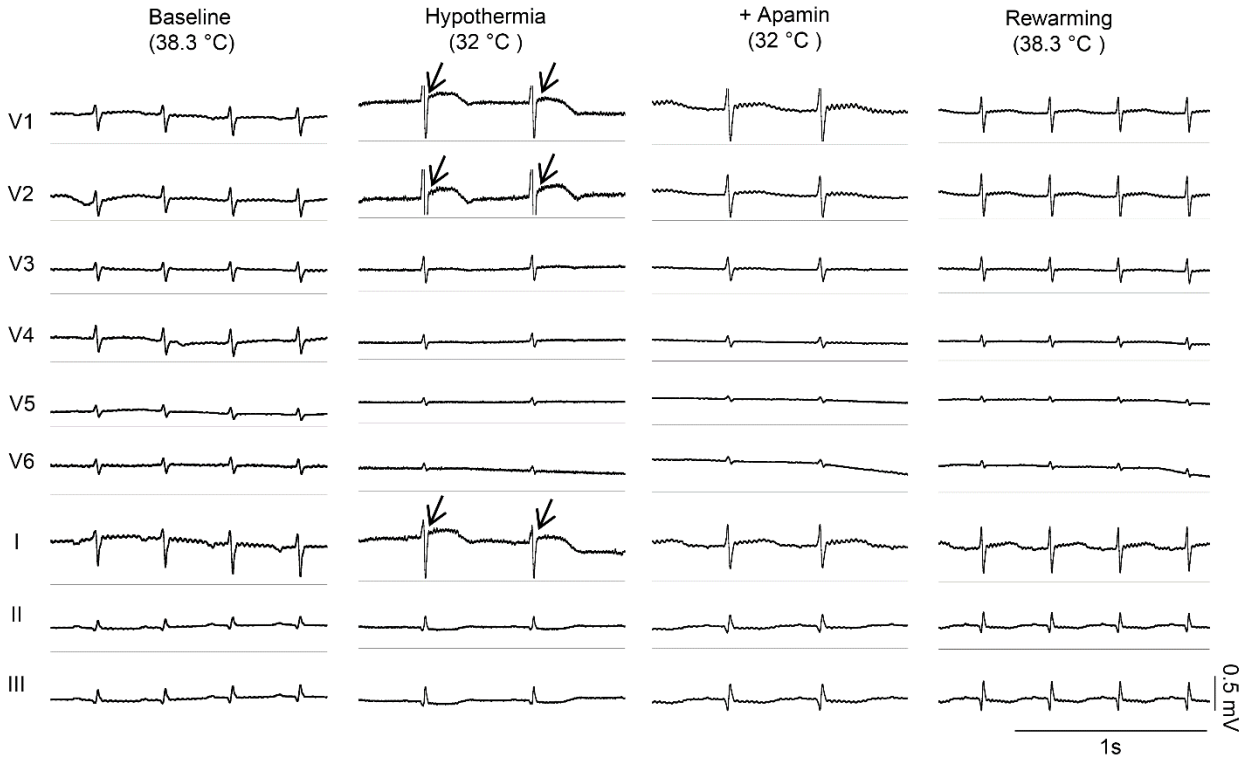

Supplemental Figure 10. I_{KAS} blockade suppresses Osborn waves in vivo. Figures show representative recordings of continuous surface ECG in an anesthetized rabbit. No J wave was observed at baseline (38.3 °C). Hypothermia (32 °C) induced J point elevation in Leads V1, V2 and I (arrow). Subsequent apamin administration (at 32 °C) suppressed J wave. After rewarming to 38.3 °C, no J wave was observed.

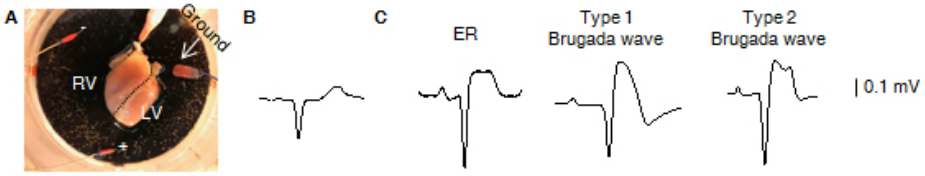

Supplemental Figure 11. Definitions of J waves in pECG. A. Electrodes arrangement for pECG recording in Langendorff perfused rabbit hearts. **B.** pECG at baseline. **C.** Representative pECG of early repolarization (ER), Type 1 Brugada wave and Type 2 Brugada wave.

Supplemental Table 1 Effects of CyPPA on I_{Na} in rabbit ventricular cardiomyocytes

	Control	CyPPA (10 µmol/L)	n
I_{Na}			
At -40 mV (pA/pF)	-47.6 ± 6.3	-21.9 ± 3.0 *	11
Activation			
V_h (mV)	-58.1 ± 0.8	-58.9 ± 1.1	6
k	2.3 ± 0.2	2.1 ± 0.3	
Inactivation			
V_h (mV)	-65.7 ± 0.9	-67.9 ± 1.5	6
k	2.1± 0.7	2.2 ± 0.4	
Recovery			
τ (ms)	42.8 ± 6.9	69.2 ± 11.0 *	6
Capacitance (pF)	126.8 ± 7.2	131.3 ± 10.6	11

V_h, membrane potential for half-maximal (in)activation; k, the slope factor; τ (tau), time constant of recovery from inactivation; n, cell numbers. * $p<0.05$. Data represent mean ± SEM. Statistical significance was determined by paired Student's t tests.

Supplemental Table 2 Comparisons among BrS, ERS and CyPPA-induced JWS

	BrS (1)	ERS (1)	CyPPA-induced JWS	Possible mechanisms for CyPPA-induced JWS
Male predominance	Yes	Yes	Males develop more episodes of SVF. ES occurs only in males.	The activation of SK3-mediated I_{KAS} is more heterogeneous in males than in females.
Region most involved	RVOT	LV inferior wall	RV	The activation of SK3-mediated I_{KAS} is more heterogeneous in the RV than in the LV.
ECG leads affected	V1-V3	II, III, aVF; V4, V5, V6; I aVL	pECG	
ECG Dynamicity	Yes	Yes	Yes	Chaotic properties; Possible intrinsic autonomic modulation of I_{KAS}.
SVF/SVT trigger	Short-coupled PVC	Short-coupled PVC	Short-coupled PVC or directly from sinus beats	Heterogeneously activation of I_{KAS} facilitates P2R.
Atrial arrhythmias	Yes	Yes	Yes	SK channels are highly expressed in atrium (2, 3).
conduction system abnormalities	Yes. Overlap syndromes with conduction defects and sinus node dysfunction.		Bradycardia, atrioventricular block, intraventricular conduction delays.	I_{Na} blockade. Direct effects of I_{KAS} activation. I_{KAS} is abundant in conduction systems (4-6). SK3 overexpression mice had severe cardiac conduction defects (7).
Ameliorative response to isoproterenol	Yes	Yes	Yes	Isoproterenol leads to shorter but more homogeneous APD distributions and faster conduction.

BrS: Brugada syndrome; ERS: early repolarization syndrome; JWS: J wave syndrome; SVF: spontaneous ventricular fibrillation; ES: electrical storm; RVOT: right ventricular outflow tract; LV: left ventricle; SVT: spontaneous ventricular tachycardia; PVC: premature ventricular contraction; P2R: phase 2 reentry; APD: action potential duration

Supplemental references

1. Antzelevitch C, Yan GX, Ackerman MJ, Borggrefe M, Corrado D, Guo J, et al. J-Wave syndromes expert consensus conference report: Emerging concepts and gaps in knowledge. *Heart Rhythm.* 2016;13(10):e295-324.
2. Lu L, Zhang Q, Timofeyev V, Zhang Z, Young JN, Shin HS, et al. Molecular coupling of a Ca^{2+}-activated K^+ channel to L-type Ca^{2+} channels via alpha-actinin2. *Circ Res.* 2007;100(1):112-20.
3. Tuteja D, Rafizadeh S, Timofeyev V, Wang S, Zhang Z, Li N, et al. Cardiac small conductance Ca^{2+}-activated K^+ channel subunits form heteromultimers via the coiled-coil domains in the C termini of the channels. *Circ Res.* 2010;107(7):851-9.
4. Zhang Q, Timofeyev V, Lu L, Li N, Singapuri A, Long MK, et al. Functional roles of a Ca^{2+}-activated K^+ channel in atrioventricular nodes. *Circ Res.* 2008;102(4):465-71.
5. Reher TA, Wang Z, Hsueh CH, Chang PC, Pan Z, Kumar M, et al. Small-Conductance Calcium-Activated Potassium Current in Normal Rabbit Cardiac Purkinje Cells. *J Am Heart Assoc.* 2017;6(6):e005471.
6. Torrente AG, Zhang R, Wang H, Zaini A, Kim B, Yue X, et al. Contribution of small conductance K^+ channels to sinoatrial node pacemaker activity: insights from atrial-specific Na^+ /Ca^{2+} exchange knockout mice. *J Physiol.* 2017;595(12):3847-65.
7. Mahida S, Mills RW, Tucker NR, Simonson B, Macri V, Lemoine MD, et al. Overexpression of *KCNN3* results in sudden cardiac death. *Cardiovasc Res.* 2014;101(2):326-34.